Urban Forestry & Urban Greening 31 (2018) 109–119

Contents lists available at ScienceDirect

Urban Forestry & Urban Greening

journal homepage: www.elsevier.com/locate/ufug

Mapping the spatial distribution of shade provision of street trees in Boston using Google Street View panoramas

Xiaojiang Li*, Carlo Ratti

MIT Senseable City Lab, Department of Urban Studies and Planning, Massachusetts Institute of Technology, Room 9-250, 77 Massachusetts Avenue, Cambridge, MA, 02139, United States

A R T I C L E I N F O

Keywords:
Google Street View (GSV)
Sky view factor
Shade provision
Street trees

A B S T R A C T

Street trees provide shade and increase human thermal comfort during hot summer. In this study, we investigated the spatial distribution of shade provision of street trees in Boston, Massachusetts. The sky view factor (SVF), which influences the solar radiation to the ground and affects human thermal comfort, was used to indicate the contribution of street trees on shade provision. Google Street View (GSV) panoramas were used to calculate the photographic method based SVF (SVF_P), with the consideration of all kinds of obstructions within street canyons. A building height model was used to calculate the simulation based SVF (*SVFs*), with consideration of obstruction of building blocks only. Considering the fact that street trees and building blocks are the two major obstructions of radiation within street canyons, therefore, the difference between the two SVF estimation results can be considered as the shade provision of street trees. The results show that street trees help to decrease the SVF by 24.61% in Boston, Massachusetts. The shading level varies spatially in the study area. Generally, the southwestern area has much higher shading level than the north and the east. We further explored the shading variation among different socioeconomic groups in the study area. Result shows that Hispanics tend to live in neighborhoods with lower shading level. This study can help to provide a reference for future urban greening projects for global climate change adaption.

1. Introduction

Thermal comfort in cities has become more and more important, especially in the context of global warming and rapid urbanization (Kong et al., 2016; Luber and McGeehin, 2008; Sanusi et al., 2016; Yuan et al., 2017). Urban thermal comfort would influence human outdoor activities and the utilization of urban space (Huang et al., 2015; Hwang et al., 2011). Severe heat has negative impacts on human well-being and efficiency (Lee et al., 2013). In the United States, extreme heat events are responsible for about one-fifth of natural hazard deaths (Borden and Cutter, 2008). With the rise in global warming, many cities are expected to experience more severe heat waves (IPCC, 2007). The urban heat island effect would cause additional warming to the urban areas (Estrada et al., 2017; Mills, 2014). This additional warming caused by urban heat island effect could bring 2.6 times more economic costs of climate change to cities (Estrada et al., 2017). In cities, the street is the basic unit and a focal point of human activity, acting as the foundation for transportation and information exchange (Li et al., 2017). City streets become one of the most critical urban landscape features affecting, or reflecting, people's lifestyles and physical, mental, and social well-beings (Miller and Tolle, 2016). Designing more thermally comfortable streets has become more and more important.

As an integral part of urban ecosystems, street trees help to regulate urban microclimates and mitigate urban heat islands (Chen et al., 2006; Onishi et al., 2010; Richards and Edwards, 2017; Sanusi et al., 2016). In hot summers, street tree canopies can block the sunlight from radiating to the ground directly and provide shade for pedestrians. However, we should also note that the cooling effects might be counter-balanced at night, as trees can trap heat and reduce ventilation at night (Coutts et al., 2016; Salmond et al., 2016). Using urban greening projects is an effective method to increase human thermal comfort in cities without changing the existing built environment (Armson et al., 2013; Coutts et al., 2016; Klemm et al., 2015).

Accurate assessment of the shading service provided by street trees must be guaranteed for urban greening projects. Remotely sensed tree canopy cover has been widely used to evaluate the amount of street trees (Landry and Chakraborty, 2009; MacFaden et al., 2012). However, two-dimensional cover information cannot fully reflect the shading service of street trees. This is because the tree canopy cover does not include the information of density and vertical structure of the

* Corresponding author.
E-mail address: xiaojian@mit.edu (X. Li).

https://doi.org/10.1016/j.ufug.2018.02.013
Received 9 May 2017; Received in revised form 25 January 2018; Accepted 25 February 2018
Available online 06 March 2018

trees, both of which influence the solar radiation to the ground. Richards and Edwards (2017) used Google Street View images to estimate the amount of annual diffuse and direct solar radiation that were shaded by street trees. However, the estimated shaded solar radiation is caused by the obstruction of the street trees and building blocks combined. In addition, the amount of solar radiation varies in different cities. In this study, we used the sky view factor (SVF) to measure the shading effectiveness of street trees alone. As a dimensionless parameter of the urban geometry, the SVF represents the ratio between the radiation received by a planar ground and that from the entire hemispheric input radiation (Watson and Johnson, 1987). The SVF value ranges from 0 to 1, which indicates totally enclosed and totally open street canyons, respectively. The SVF has been widely used to represent the shade provision of street trees (Lin et al., 2012; Lee et al., 2013; Hwang et al., 2011).

There are many developed methods to calculate the SVF. The photographic method and the building height model based simulation method are the two most widely used methods for SVF estimation. The photographic method is a classical method for estimating SVF (Steyn, 1980). Hemispherical images taken in fieldworks are required to estimate the SVF in the photographic method. Sky areas are first delineated from the hemispherical image and the binary sky image is further divided into annuli. The SVF is then calculated as the sum of all sky fractions in all annuli. Since the hemispherical image presents the obstruction of building and tree canopies, therefore, precise estimation of SVF can be attained using the photographic method. However, it is difficult to separate the obstruction effects of street trees and building blocks on solar radiation.

The building height model based simulation method estimates the SVF based on the simulation of light radiation on the ground (Gal et al., 2009; Ratti and Richens, 2004). A building height model is usually used to represent the ground surface, and the canopy cover is also included sometimes. However, the 3D structure of the canopy is difficult to derive and it is difficult to consider the 3D structure in calculating the SVF in the simulation method. Therefore, the SVF result calculated by the simulation method usually considers the obstruction of building blocks alone (Chen et al., 2012; Ratti and Richens, 2004).

In this study, we used two different methods to estimate the SVF values in Boston, Massachusetts to focus specifically on the shading effectiveness of street trees. We generated hemispherical images from GSV panoramas by geometrical transformation to replace the *in situ* hemispherical images to calculate the photographic method based SVF (SVF_P). We further calculated the simulation method based SVF (SVF_S) using building height models in the study area. The simulation method tends to overestimate the SVF values because the obstruction of street trees is not considered. The photographic method can get the precise SVF estimation result. Therefore, the SVF difference ($SVF_S - SVF_P$) between these two methods is caused by street trees, which can also be used to indicate the shade provision of street trees.

2. Study area and data

As the largest city in both Massachusetts and New England, Boston was chosen as the study area (Fig. 1). According to recent census data (American Census Survey 2009–2014 data), Boston has a total population about 660,000. The study area has varied street canyon types, which range from skyscrapers in the downtown area and the low-lying residential area in the periphery areas (Fig. 1(a)).

The datasets used in this study include building footprint maps, land use maps, LiDAR data, tree canopy data, and the street maps of Boston. The LiDAR data was downloaded from NOAA Digital Coast (https://coast.noaa.gov/dataviewer/#/lidar/search/), with the horizontal accuracy of 50 cm and vertical accuracy of 15 cm. We further generated the digital surface model (Fig. 1(a)) based on the first echo data of the LiDAR data. The building footprint map and land use map in the study area were collected from MassGIS (https://www.mass.gov/orgs/massgis-bureau-of-geographic-information). The original land use map includes 31 land use types in the study area. In order to facilitate further analysis, we aggregated similar land use types in the original land use map into several major land use types: commercial land, industrial land, recreational land, and residential land. Table 1 shows the descriptions of four aggregated land use types.

The tree canopy data of Boston (Fig. 1(b)) was from Raciti et al. (2014), which was delineated from 0.5 m resolution digital orthoimagery with an overall accuracy of 95%. Based on the street map (Fig. 1(c)) in the study area, we collected 12,153 GSV panoramas along streets. Street trees change colors in different seasons, which may further influence our analysis. Based on the visual appearance of street trees in different seasons (Fig. 2(a)), we defined the leaf-on season in Boston as of June, July, August, and September. However, it is difficult to define May as leaf-on season or leaf-off season. Fig. 2(a) shows that trees are green in May 2014 and tend to leafless in May 2016. This is probably because those GSV panoramas taken in May 2014 were taken in late May, but those panoramas taken in 2016 were taken in early May. We further checked all the panoramas taken in May of different years, and we included the panoramas taken in May 2014 in the following analyses. GSV panoramas that were taken during leaf-off season or in the tunnels were removed from further analysis. Finally, we used 11,451 GSV panoramas in Boston. By checking the spatial patterns of green GSV sites distribution (Fig. 2(b)), we found that the panorama sites are suitable to represent the whole study areas, although there is a small portion of the study area that has no GSV panorama sites. More details about the GSV panorama collection are described in the following section.

3. Methodology

3.1. Google Street View (GSV) panorama collection

GSV panoramas can be requested by inputting coordinates through Google's Application Programming Interface (API). Fig. 3 shows one example of requested GSV panorama tiles and the mosaicked GSV panoramas. Each GSV panorama tile can be requested using the corresponding uniform resource locator (URL). In the URL address, the *panoid* represents the unique panorama ID, *x* and *y* represent the column and row number of the tile in the corresponding panorama, and *zoom* represents the zooming scale of the GSV panorama. In this study, the IDs and date information of the panoramas were requested using the method from Li et al. (2016) based on the input coordinates. We further developed a Python script (See code in Appendix A) to download the left and right tiles and mosaic them to a complete panorama automatically for each site using the panoramas ID as input.

3.2. Photographic method for sky view factor (SVF) estimation

The SVF represents the ratio between the solar radiation received by a planar ground and that from the entire hemispheric input radiation. The SVF value ranges from 0 to 1, which indicates totally enclosed and totally open street canyons, respectively. The photographic method based on hemispherical images is a widely used method for sky view factor (SVF) estimation. In the photographic method, the obstruction effects of building blocks and tree canopies are considered. In this study, hemispherical images were generated from GSV panoramas based on the geometrical model (Fig. 4) between the cylindrical projection and azimuthal projection (Li et al., 2017). Any pixel (x_c, y_c) in GSV panoramas can be projected to the corresponding pixel (x_f, y_f) in the hemispherical images based on the geometrical model (Fig. 4).

The automatic image classification is a requisite step for the automatic SVF calculation in the photographic method based on GSV panoramas. Considering the fact that both the building blocks and tree canopies act as obstructions of the sky, we classified the hemispherical images into three classes: sky pixels, vegetation pixels, and building

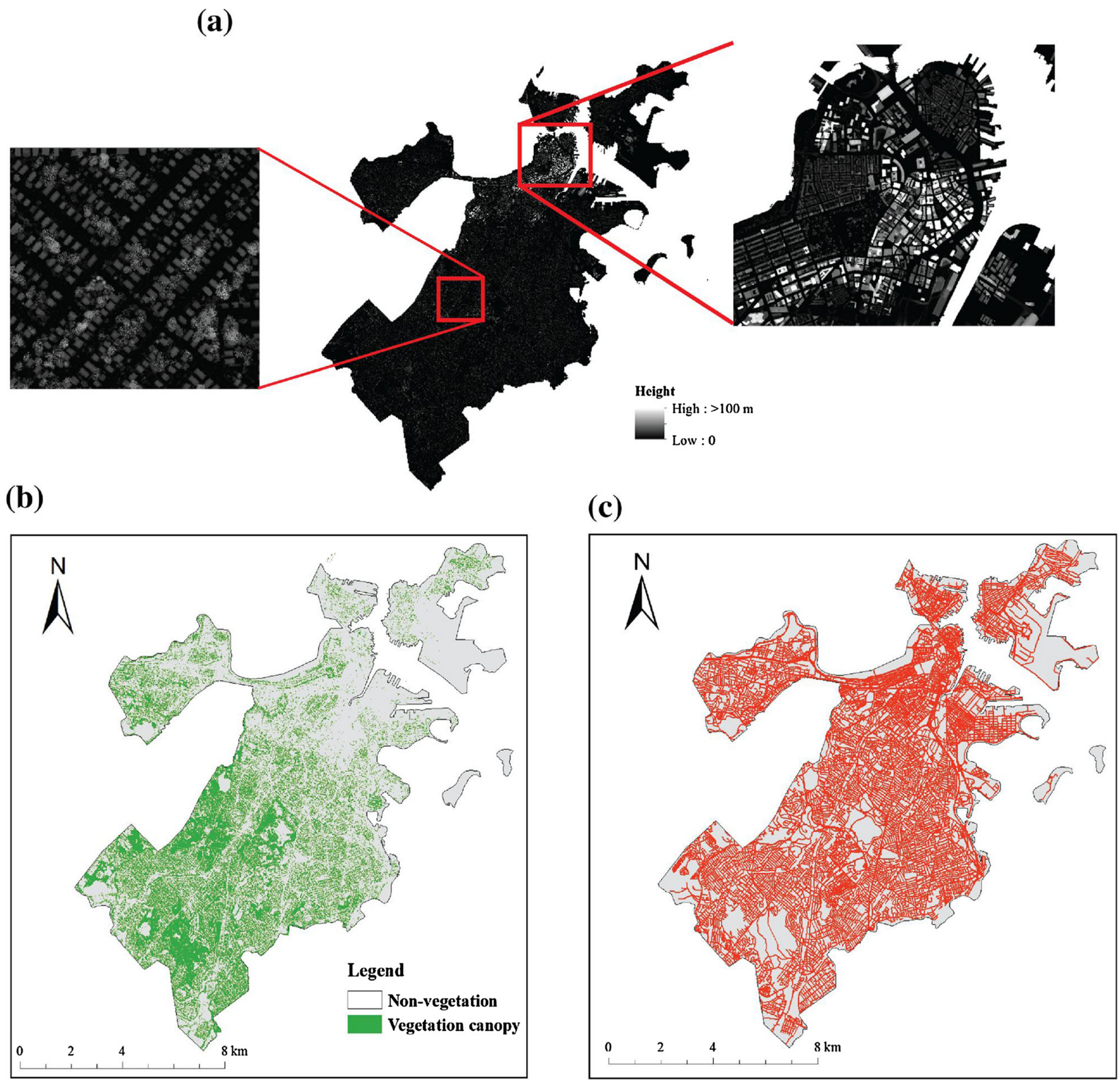

Fig. 1. The location and maps of the study area, (a) the digital surface model derived from LiDAR, (b) the vegetation canopy cover (green part), (c) the street map of Boston. (For interpretation of the references to color in this figure legend, the reader is referred to the web version of this article.)

Table 1
The aggregated land use types in Boston and the description of each land use type.

Land use types	Descriptions
Commercial land	Malls, shopping centers and larger strip commercial areas, plus neighborhood stores and medical offices (not hospitals).
Industrial land	Light and heavy industry, including buildings, equipment and parking areas; transportation land; mining; transitions.
Recreational land	Lands comprising open land, institutional facilities, wetlands, marina, pasture, public open green spaces, and cropland.
Residential land	High-density residential land, medium density residential, multifamily residential land.

pixels. In this study, we first used the mean-shift segmentation algorithm to aggregate nearby pixels that have similar spectral information together in the hemispherical images (Comaniciu and Meer, 2002; Li et al., 2015a,b). Fig. 4(c) shows a segmented image based on mean-shift algorithm. Compared with the original hemispherical image (Fig. 4(b)), the segmented image is composed of homogeneous polygons that are physically meaningful, which would be more suitable for image classification.

Different from the sky and building pixels, the tree canopy pixels show as green in the hemispherical images. Therefore, in this study, we used the *ExG* ($2 \times green - blue - red$) to enhance the difference between the vegetation pixels and non-vegetation pixels. The sky pixels are usually brighter than non-sky pixels and have higher reflectance on the blue channel. Therefore, we used a modified brightness, which gives more weight to the blue band and less weight to the red band, to extract the sky pixels. The modified brightness is calculated as,

$$Brightness = (red + green + 2 \times blue)/3 \quad (1)$$

where *red*, *green*, and *blue* are the pixel values in red, green, and blue bands, respectively. The pixels with higher *Brightness* values are sky pixels. We further used Otsu's method (Otsu, 1975) to find optimum thresholds to separate the sky pixels from the non-sky pixels based on the calculated *Brightness* images, and to extract the vegetation pixels based on the *ExG* images. The Otsu's method can find a global threshold automatically with minimum within-class variance and maximum between-class variance. All other pixels other than sky and vegetation were treated as building pixels.

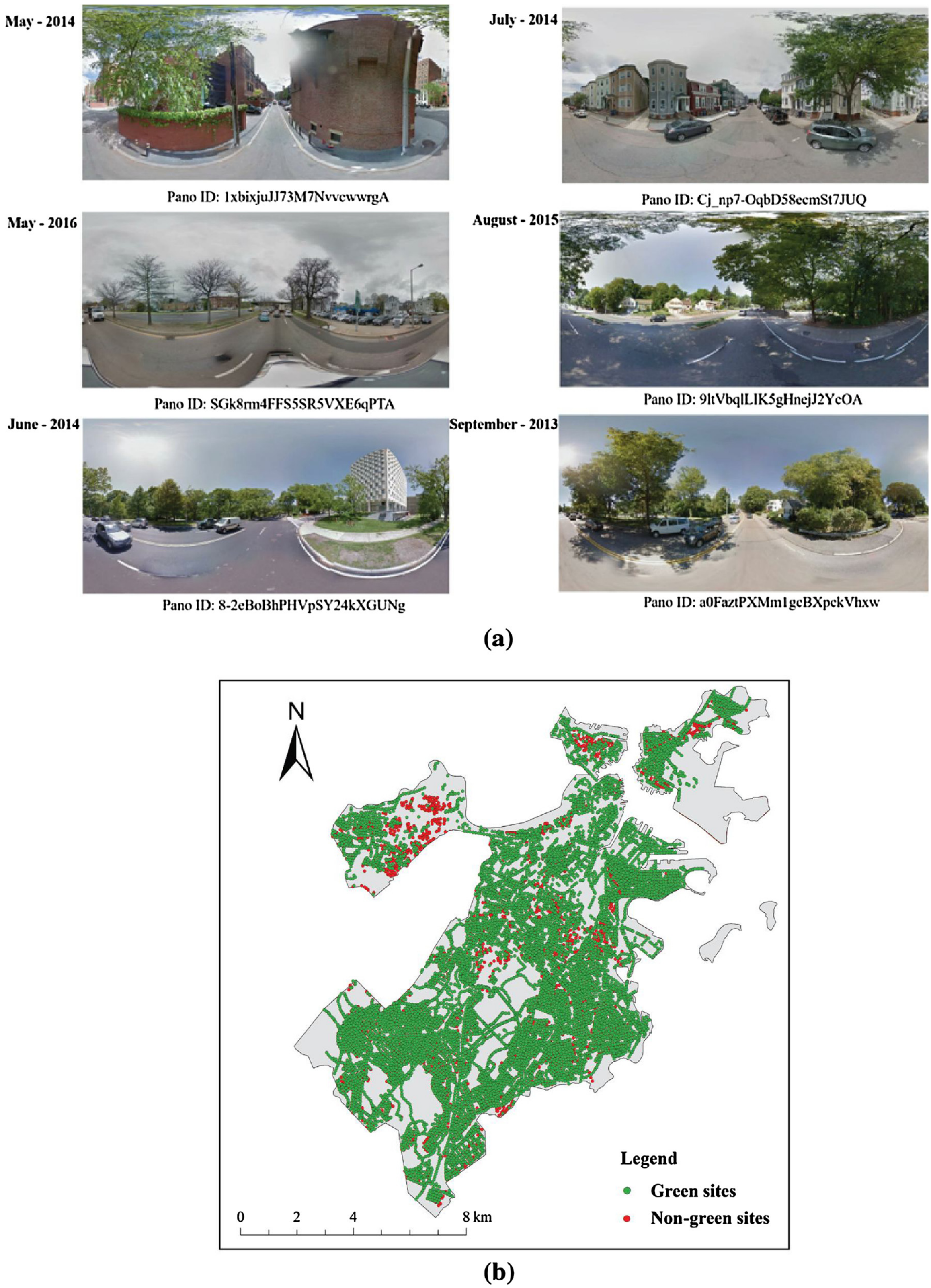

Fig. 2. Selecting GSV panoramas in leaf-on season, (a) GSV panoramas in different months, (b) the spatial distribution of GSV panorama sites – the green dots represent the panoramas taken in leaf-on season and the red dots represent GSV panoramas taken in leaf-off season. (For interpretation of the references to color in this figure legend, the reader is referred to the web version of this article.)

In order to refine the sky classification results, we further applied geometrical rules to the preliminary sky classification results, such as sky pixels should be above the building pixels, the center of the hemispherical images should be sky pixel or vegetation pixels. Fig. 4(d) shows the sky classification result on a hemispherical image based on the above spectral and geometrical rules.

Based on the sky classification results, we further applied the classical photographic method to calculate the SVF_P. The photographic

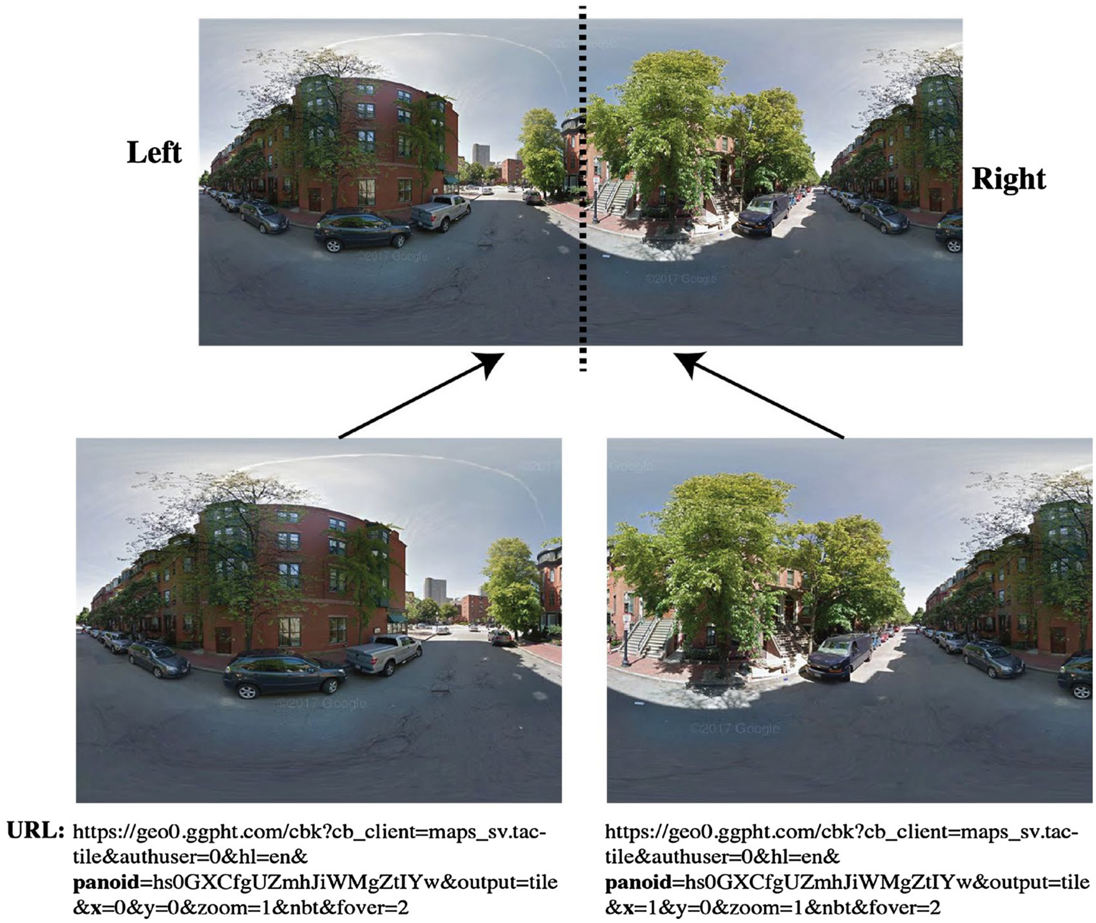

Fig. 3. A GSV panorama and its two tiles together with their corresponding URLs.

method first creates n (here is set to 37) annular rings on sky images. The SVF_P is then calculated as the sum of all sky fractions in all annuli (Johnson and Watson, 1984),

$$SVF_P = \frac{1}{2\pi}\sin\left(\frac{\pi}{2n}\right)\sum_{i=1}^{n}\sin\left(\frac{\pi(2i-1)}{2n}\right)\alpha_i \tag{2}$$

where i is the ring index, n is the number of rings, and α_i is the angular width in ith ring.

3.3. Estimation of shade provision of street trees

In the photographic method, the calculated SVF_P considers the obstruction of both the building blocks and tree canopies. In order to split the obstruction effect of building blocks and estimate the shade provision of street tree canopies, we further calculated the SVF_S contributed by the building blocks only using the simulation method based on the building height model of the study area. The building height model was created by overlaying the building footprint map on the digital surface model that was derived from LiDAR data. Based on the building height model, the simulation based SVF_S can be calculated as:

$$SVF_S = 1 - \frac{1}{360}\sum_{\alpha=0}^{359}\sin^2\beta_\alpha \tag{3}$$

where β_α is the maximum angle of the obstruction building at the horizontal direction of α, and α ranges from 0 to 359. Considering the fact that GSV panoramas are not taken at the zero height ground, but at height of 2.5m, we revised the simulation method by using a modified β_α to make the simulation method and photographic method comparable. The modified β_α is calculated as:

$$\beta_\alpha = \arctan\frac{H_\alpha - 2.5}{D_\alpha} \tag{4}$$

where H_α is the building height at the horizontal direction of α with the maximum angle of the obstruction, and α ranges from 0 to 359; D_α is the distance between the building and panorama site.

The simulation method calculates the SVF_S based on the simulation of light radiation in the building height model with the obstruction effect of tree canopies not considered. Therefore, the SVF_S tends to overestimate the SVF values compared with the SVF_P. Fig. 5 shows the different open sky areas estimated by the GSV based photographic method and the building height model based simulation method (Fig. 5(b)). Therefore, the shading effectiveness of the street trees can be estimated as the difference between the photographic based SVF (SVF_P) and the simulation method based SVF (SVF_S):

$$\text{SVF difference} = SVF_S - SVF_P \tag{5}$$

The SVF difference indicates the actual shading effectiveness of the street trees, which equals to the amount of shade provision of street trees without the overlap part with the shade provision of building blocks.

3.4. Analyzing the distribution of shade provision

In order to investigate the connection between the physical environment of streetscapes and the shade provision of street trees, we conducted correlation analyses between the shade provision of street trees (*SVF* difference) and streetscape built environment variables for all 11,451 GSV sites. In addition, we analyzed the shade provision of street trees in different relatively homogeneous land use types,

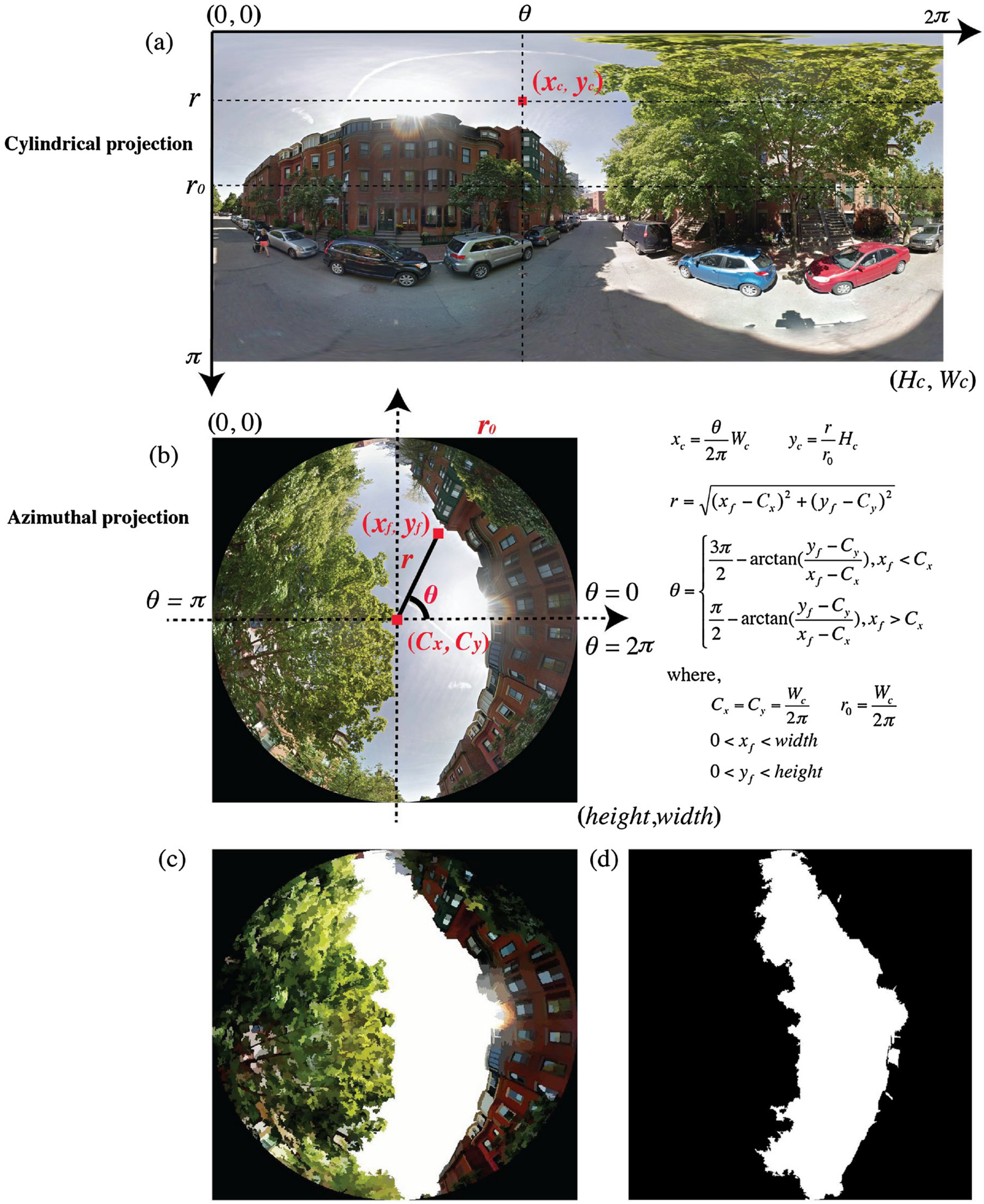

Fig. 4. Using GSV panorama for SVF_P estimation, (a) a cylindrical GSV panorama, (b) the generated hemispherical image based on the geometrical transform model, (c) the segmented image based on mean-shift algorithm, (d) the sky pixels classification result for one hemispherical image.

commercial land, industrial land, recreational land, and residential land. The SVF_S values, SVF_P values, and shade provision (SVF difference) were compared between different land use types using ANOVA analysis. Three physical environment variables, percentage of tree canopy cover (PCC), averaged tree canopy height (ACH), and averaged building height (ABH), were calculated to indicate the surrounding physical streetscape environment. These three variables were calculated at a buffer distance of 20 m around the GSV sites based on the building height model and tree canopy map in the study area.

We further conducted correlation analyses between the shade provision and the socioeconomic variables. Based on previous studies (Huang et al., 2011; Li et al., 2015b), we chose nine socioeconomic variables at census tract level to indicate the socioeconomic status of local residents. These social variables are, per capita income, percentage of people without high school degree, percentage of people with bachelor or higher degree, percentage of owner-occupied house units, percentage of non-Hispanic Whites, percentage of Hispanics, percentage of African Americans, percentage of people younger than 18 years old, and percentage of people older than 65 years old. All these variables were derived from American Census Survey 2014 5-year data.

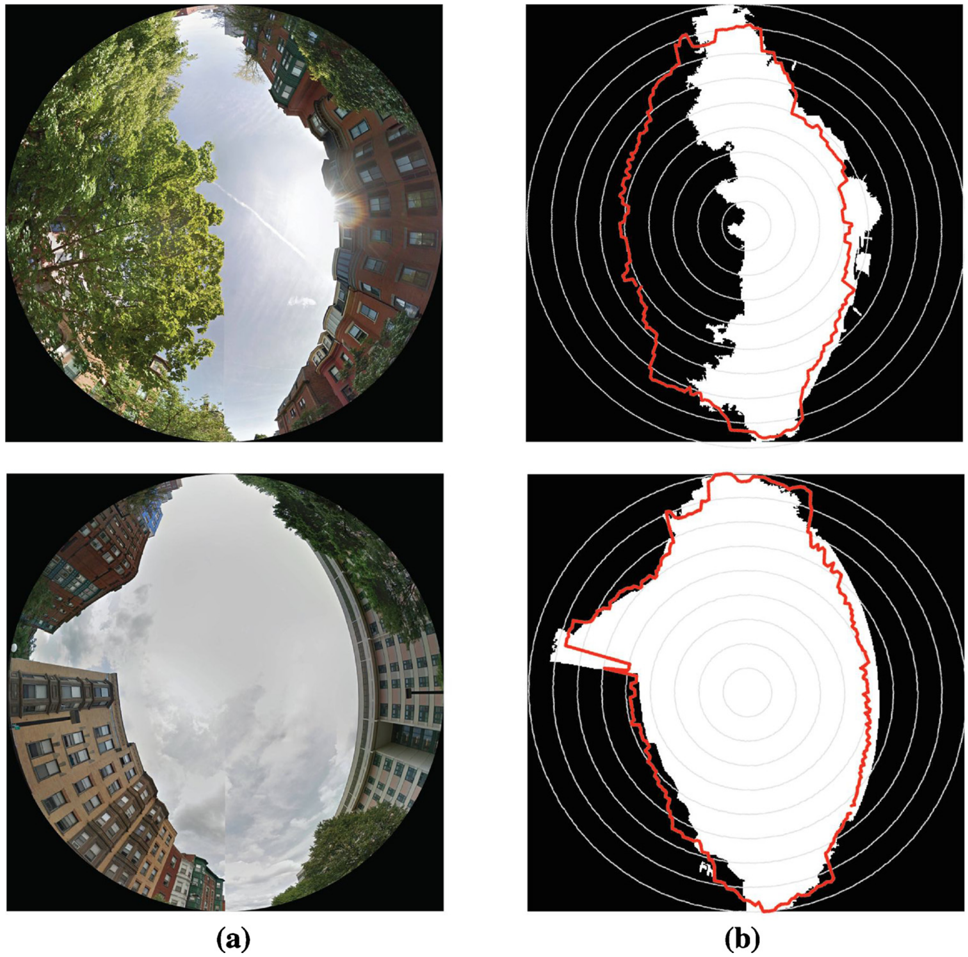

Fig. 5. Hemispherical images created by GSV panoramas and building height model. (a) hemispherical images created by GSV panoramas, (b) the overlay of open sky areas estimated based on the GSV panorama method (white region), and open sky areas estimated by the simulation method using the building height model (region encircled by red line). (For interpretation of the references to color in this figure legend, the reader is referred to the web version of this article.)

4. Results

Fig. 6 shows the spatial distributions of the simulation based SVF (SVF_S) and the photographic based SVF (SVF_P) in Boston. In the *SVFs* map (Fig. 6(a)), it is obvious that the SVF_S values in the periphery areas are much higher than in the downtown area (bound by black box in Fig. 6). This is because the high-rise buildings in the downtown area (Fig. 1(a)) would obstruct the sky area and further decrease the SVF_S values significantly. The distribution of SVF_P (Fig. 6(b)) has a very different spatial pattern compared with the distribution of SVF_S. The SVF_P was calculated based on the hemispherical images transformed from GSV panoramas. Therefore, the SVF_P represents the SVF values with consideration to obstruction of building blocks and street tree canopies. Similar with the SVF_S, downtown areas also have low SVF_P because of the high-rise buildings there. Different from the SVF_S distribution, in the SVF_P map (Fig. 6(b)), the periphery parts also have relatively low SVF values. Although the distributions of SVF_P and SVF_S have very different spatial patterns (Fig. 6), both SVF_P and SVF_S values are low in downtown areas.

The difference of SVF_P and SVF_S (Fig. 6(c)) indicates the contribution of street trees on solar radiation obstruction, which also represents the shade provision of street trees. Generally, the southern and the western parts of the study area have larger SVF difference. Compared with the tree canopy map (Fig. 6(d)), we can see a similar pattern between the SVF difference and the tree canopy map. Sites with more tree canopy cover tend to have larger SVF difference. This can be further proved by the correlation analysis results between the shade provision of street trees (SVF difference) and surrounding built environment variables, percentage of tree canopy cover (PCC), averaged tree canopy height (ACH), and averaged building height (ABH). Table 2 presents the correlation analysis results between the SVF difference and PCC, ACH, ABH in 20 m buffer zone around 11,451 GSV sites. The PCC and ACH both have significant positive correlations with the SVF difference values (PCC: $r = 0.136$; ACH: $r = 0.650$). The ABH has a significant and negative correlation with the SVF difference (ABH: $r = -0.168$). The similar correlations were also found between the shade provision and three built environment variables in different land use types (Table 2). This is because more tree canopy cover and larger canopy height tend to provide more shade, and the shade provision of high-rise buildings will cover the shade provision of street trees and decrease the shading effectiveness of street trees.

Different land use types have different amounts of street tree providing shade. Among the 11,451 GSV panorama sites in the study area, 7224 sites are located on residential land, 1791 sites on recreational land, 1309 sites on commercial land, and 1127 sites on industrial land. Fig. 7 presents the box plots of SVF_P, SVF_S, and *SVF* difference values for different land use types in the study area. ANOVA analysis results show that the SVF_P values in industrial land (Mean = 0.80, Std = 0.18) are higher than SVF_P values in other land use types significantly ($t = 23.62$, $p < 0.001$). Similar with the SVF_P, the SVF_S values in the industrial land are larger than other land use types ($t = 9.23$, $p < 0.001$). The SVF_S difference among different land use types is smaller than the SVF_P difference. The amount of shade provision of street trees varies in different land use types (Fig. 7(c)). Generally, street trees in recreational

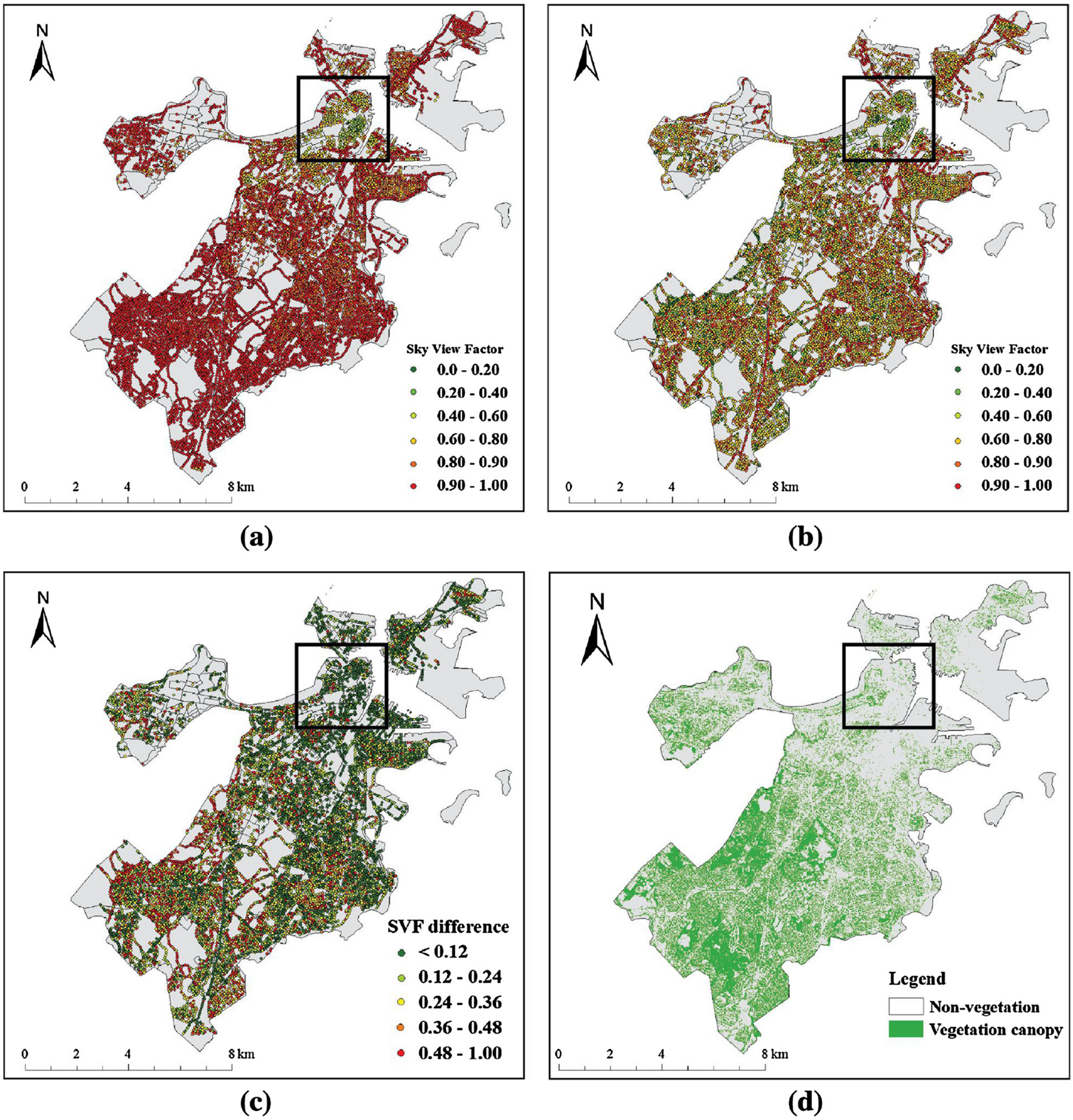

Fig. 6. The spatial distributions of SVF_S and SVF_P in Boston (the black box marks the downtown areas), (a) the spatial distribution of SVF_S calculated based on building height model, (b) the spatial distribution of SVF_P calculated based on Google Street View panoramas, (c) the spatial distribution of the SVF difference ($SVF_S - SVF_P$), (d) the tree canopy cover in the study area.

Table 2
The correlation between shade provision (SVF difference) and three built environment variables in 20 m buffer zone of GSV sites, PCC represents percentage of canopy cover, ACH represent average canopy height, and ABH represents the average building height.

Land uses	Pearson's correlation coefficients		
	PCC	ACH	ABH
All land use (N = 11,451)	0.136[a]	0.650[a]	−0.168[a]
Commercial land (N = 1309)	0.276[a]	0.611[a]	−0.291[a]
Industrial land (N = 1127)	−0.001	0.393[a]	−0.142[a]
Recreational land (N = 1791)	0.173[a]	0.738[a]	−0.274[a]
Residential land (N = 7224)	0.209[a]	0.618[a]	−0.146[a]

[a] Correlation is significant at the 0.01 level (2-tailed).

land (Mean = 0.27, Std = 0.24) and residential land (Mean = 0.25, Std = 0.22) provide more shade than commercial land (Mean = 0.13, Std = 0.16) and industrial land (Mean = 0.14, Std = 0.16) in Boston.

The point level shade provision map was further aggregated to census tract level by mean value in order to check the spatial pattern and compare with socioeconomic variables. Fig. 8 shows the spatial distribution of the percentage of SVF difference (shade provision of street trees) caused by street trees in different census tracts of Boston. Overall, street trees help to decrease SVF by 24.61% (min: 1.49%, max: 47.39%) in the study area. It can be seen clearly that the southern and southwestern parts of the study areas have more shade provision of street trees than the northern and eastern parts of the study area. Table 3 summarizes the correlation analysis results between the shade provision of street trees and nine socioeconomic variables derived from census data at census tract level. The correlation results show that per capita income is not significantly correlated with the amount of shade

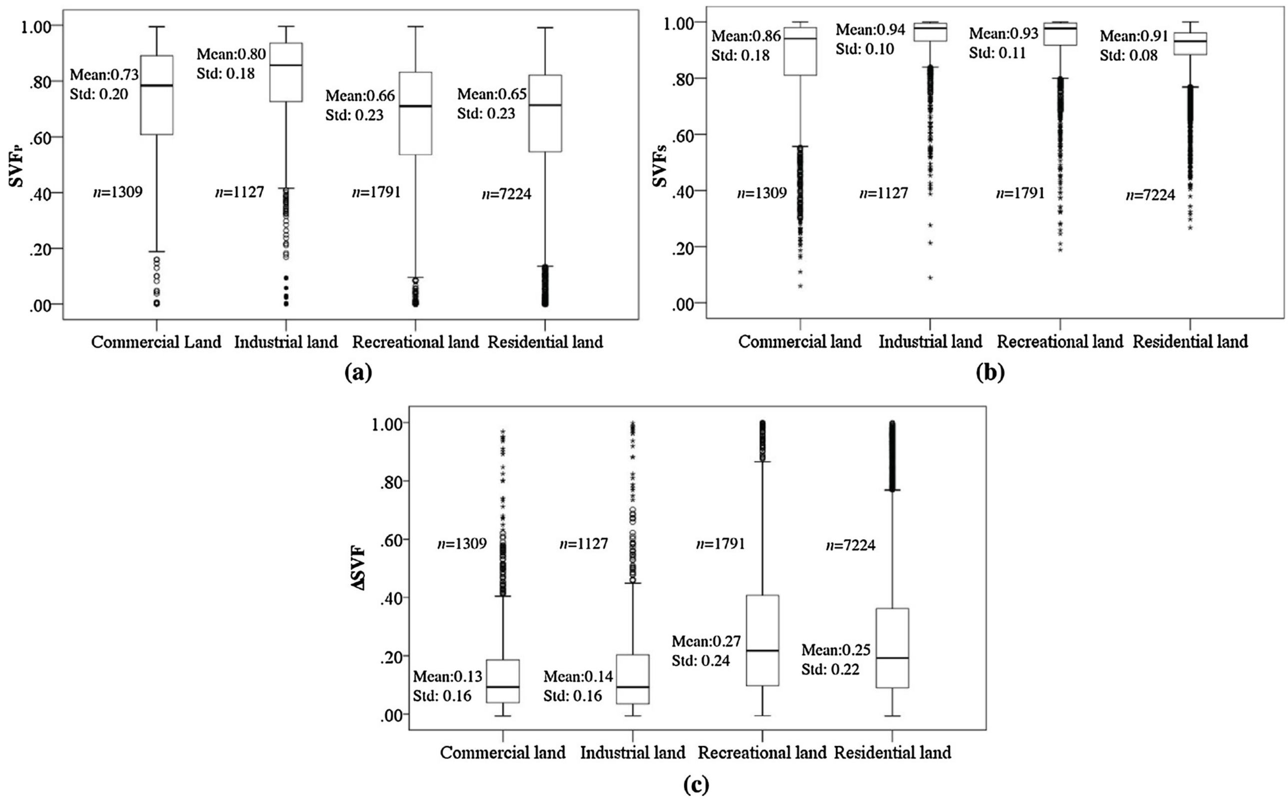

Fig. 7. Box plots of SVF values in four land use types in Boston, (a) the photographic based SVF_P, (b) the simulation based SVF_S, (c) the shade provision of street trees (SVF difference).

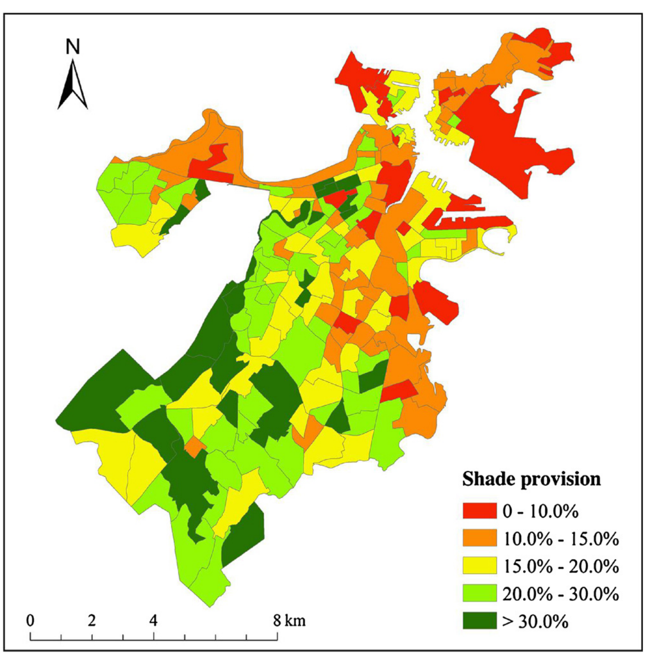

Fig. 8. The shade provision (SVF difference) of street trees in different census tracts of Boston.

provision of street trees in the study area. Those census tracts with a higher percentage of owner-occupied house units have more shade provision. People without high school degree tend to live in neighborhoods with less shade. No significant correlation was detected between the percentage of people with bachelor or higher degree and the shade provision of street trees. The percentage of Hispanics is correlated with the amount of shade provision of street trees significantly and negatively. However, both the percentage of non-Hispanic Whites and the percentage of African Americans are not significantly correlated with the shade provision of street trees. Different from the non-significant correlation between the shade provision and the percentage of people under 18 years old age, the percentage of people older than 65 years old age is significantly and positively correlated with the amount of shade provided by street trees.

5. Discussion

The study estimated the shade provision of street trees in Boston during leaf-on season by combining the Google Street View (GSV) data and remote sensing data. The dimensionless parameter of street geometry, sky view factor (SVF), was used to quantify the shade provision of street trees (Hwang et al., 2011; Lin et al., 2012). The combination of ground-level GSV panoramas and overhead view remote sensing data makes it possible to quantify the contribution of street trees alone on solar radiation obstruction within street canyons. Results show that street trees in Boston provide 24.61% of shade in the whole city, and the southwestern part of Boston has the most shade provision by street tree canopies than other regions (Fig. 6(c)). Generally, downtown areas have lower shade provided by the street trees. This is not difficult to understand, since it is difficult to plant and maintain street trees in downtown areas because of the limited space and the large pavement areas there (Dwyer et al., 1992; Nowak et al., 2004). In addition, the shade provided by the high-rise buildings would overlap and cover the shade provided by the street trees in downtown areas. The results of correlation analysis between the shade provision and the built environment variables further prove this explanation (Table 2). The correlation results show that the vegetation canopy cover and average canopy height are two major positive contributors of the shade provision, and the building height is a negative contributor of the shade provision of street trees. In periphery residential areas, the street trees provide much more shade to the local residents, which may further contribute to thermal comfort and help save energy cost during the

Table 3
The correlations between the shade provision of street trees and the socioeconomic variables derived from American Community Survey (ACS) census data.

Category	Variables	Pearson's correlations	Sig (2-tailed)	N
Economic status	Per capita income	0.167	0.027	174
Education	Percentage of people without high school degree	−0.288	−0.000[a]	
	Percentage of people with bachelor or higher degree	0.174	0.021	
Lifestyle	Percentage of owner-occupied house units	0.375	0.000[a]	
Race/Ethnicity	Percentage of non-Hispanic Whites	0.172	0.023	
	Percentage of Hispanics	−0.200	−0.010[a]	
	Percentage of African Americans	−0.019	−0.802	
Age	Percentage of people under 18 years of age	−0.102	−0.178	
	Percentage of people older than 65 years of age	0.320	0.000[a]	

[a] Correlation is significant at the 0.01 level (2-tailed).

summer (Donovan and Butry, 2009; Hwang et al., 2011; McPherson and Simpson, 2003). The shade provision of street tree canopies varies spatially within streets and among different land use types. Streets in the recreational land and residential land have more shade provided by street tree canopies than streets in the commercial and industrial land (Fig. 7). The abundant vegetation cover and low-rise buildings explains the relatively high shade provision in the residential and recreational areas, and the high-rise buildings and the limited vegetation coverage lead to lower shade provision in commercial and industrial land (Table 2).

The spatial distribution and quantitative information of shade provision of street trees would provide an important reference for urban planners and municipal governments in future urban greening projects to maximize the ecological services of street trees. Municipal governments may find critical places for future urban greening projects to mitigate urban heat islands and increase the thermal comfort of local residents. Correlation analysis shows that different racial/ethnic groups are living in neighborhoods with different shading levels in the study area. Different from non-Hispanics Whites and African Americans, the Hispanics tend to live in neighborhoods with significantly less shade in Boston. Future urban greening projects may consider giving some priorities to neighborhoods with large Hispanic communities. In the study area, older people tend to live in neighborhoods with higher shading level. Considering the fact that older people are more vulnerable to heat stress, the current situation would be beneficial to older people in Boston. The spatial distribution of the shade provision can be used as input to quantify the ecosystem services of street trees (Salmond et al., 2016; Richards and Edwards, 2017), which would help people realize the importance of street trees and making our living environment better.

This study also shows that ground level GSV data would be an important supplemental data source for urban environmental studies. Different from the overhead view remotely sensed data, ground-level hemispherical images would capture the upside-down view of urban features within street canyons. By combining remotely sensed data and ground level GSV data, it would be possible to study tree canopy structures below the tree canopies and analyze the influence of tree canopies on the solar radiation, which would be very difficult using overhead view remote sensing data alone.

In addition, this study provides a fully automatic workflow for quantifying the shade provision of street trees without much cost and computational burden. The datasets required in the proposed method of this study are easily accessible for most cities. The GSV panoramas are publicly available, and the building height model can be generated based on building footprint map and floor information from local government. All the data collection and image processing procedures can be done on a personal computer. In this study, for all 11,451 GSV panoramas in Boston, it took about 48 h to collect all GSV panoramas, process synthetic hemispherical images, and generate the shade estimation result on a 64-bit desktop computer with 8G RAM and 3.7 GHz processor. Considering the wide coverage and public accessibility of GSV data, the proposed method used in this study would be easily deployed in the other study areas where GSV service is available.

While this study investigated the shade provision of street trees in Boston, there are still some limitations that need to be solved in the future studies. Firstly, in this study, the SVF was used to represent the shade provision of street trees. Although the SVF would influence the amount of solar radiation reaching the ground, the thermal conditions in street canyons would also be influenced by wind, humidity, and other climatic parameters. This study considered only the solar radiation, the wind and air temperature were not assessed. In future studies, more parameters should be considered to investigate the connection between street trees and human thermal comfort within street canyons.

In addition, this study is focused on the shade provision of street trees during leaf-on seasons. However, the shading effectiveness of street trees would be different in different seasons. Future studies should also consider the temporal changes of the SVF values. Currently, we can only access the GSV images of specific time points but cannot access the historical GSV data based on the current Google Maps API. In the future, the seasonal change of the shade provision should also be considered.

6. Conclusions

The proposed method investigated the shade provision of street trees using GSV at a city scale. Results show that the street trees provide 24.61% shade in Boston. The shade provision distributes unevenly in Boston, and the southwestern part has more shade provision than the north and east. Recreational land and residential land have more shade provided by street tree canopies than commercial land and industrial land. In addition, the shade distributes unevenly among different socioeconomic groups and the Hispanics tend to live in neighborhoods with less shade.

The method used in this study could be used to evaluate the shade provision of street trees in different cities, considering the global availability of GSV data. The workflow used in this study is automatic, which further makes the large-scale shade provision study possible.

Appendix A

The Python script can be found in the Github repository: https://github.com/xiaojianggis/skyview.

References

Armson, D., Rahman, M.A., Ennos, A.R., 2013. A comparison of the shading effectiveness of five different street tree species in Manchester, UK. Arboric. Urban For. 39, 157–164.
Borden, K.A., Cutter, S.L., 2008. Spatial patterns of natural hazards mortality in the United States. Int. J. Health Geogr. 7 (1), 64.
Chen, X.L., Zhao, H.M., Li, P.X., Yin, Z.Y., 2006. Remote sensing image-based analysis of the relationship between urban heat island and land use/cover changes. Remote Sens. Environ. 104 (2), 133–146.
Chen, L., Ng, E., An, X., Ren, C., Lee, M., Wang, U., He, Z., 2012. Sky view factor analysis

of street canyons and its implications for daytime intra-urban air temperature differentials in high-rise, high-density urban areas of Hong Kong: a GIS-based simulation approach. Int. J. Climatol. 32 (1), 121–136.
Comaniciu, D., Meer, P., 2002. Mean shift: a robust approach toward feature space analysis. IEEE Trans. Pattern Anal. Mach. Intell. 24 (5), 603–619.
Coutts, A.M., White, E.C., Tapper, N.J., Beringer, J., Livesley, S.J., 2016. Temperature and human thermal comfort effects of street trees across three contrasting street canyon environments. Theor. Appl. Climatol. 124 (1–2), 55–68.
Donovan, G.H., Butry, D.T., 2009. The value of shade: estimating the effect of urban trees on summertime electricity use. Energy Build. 41 (6), 662–668.
Dwyer, J.F., McPherson, E.G., Schroeder, H.W., Rowntree, R.A., 1992. Assessing the benefits and costs of the urban forest. J. Arboric. 18, 227.
Estrada, F., Botzen, W.W., Tol, R.S., 2017. A global economic assessment of city policies to reduce climate change impacts. Nat. Clim. Change 7 (6), 403–406.
Gal, T., Lindberg, F., Unger, J., 2009. Computing continuous sky view factors using 3D urban raster and vector databases: comparison and application to urban climate. Theor. Appl. Climatol. 95 (1–2), 111–123.
Huang, G., Zhou, W., Cadenasso, M.L., 2011. Is everyone hot in the city? Spatial pattern of land surface temperatures, land cover and neighborhood socioeconomic characteristics in Baltimore, MD. J. Environ. Manage. 92 (7), 1753–1759.
Huang, K.T., Lin, T.P., Lien, H.C., 2015. Investigating thermal comfort and user behaviors in outdoor spaces: a seasonal and spatial perspective. Adv. Meteorol. 1–11.
Hwang, R.L., Lin, T.P., Matzarakis, A., 2011. Seasonal effects of urban street shading on long-term outdoor thermal comfort. Build. Environ. 46 (4), 863–870.
IPCC, 2007. In: Solomon, S., Qin, D., Manning, M. (Eds.), Climate Change 2007: The Physical Science Basis. Contribution of Working Group I to the Fourth Assessment Report of the Intergovernmental Panel on Climate Change. Cambridge Univ. Press, New York.
Johnson, G.T., Watson, I.D., 1984. The determination of view-factors in urban canyons. J. Clim. Appl. Meteorol. 23 (2), 329–335.
Klemm, W., Heusinkveld, B.G., Lenzholzer, S., van Hove, B., 2015. Street greenery and its physical and psychological impact on thermal comfort. Landscape Urban Plann. 138, 87–98.
Kong, F., Yan, W., Zheng, G., Yin, H., Cavan, G., Zhan, W., Cheng, L., 2016. Retrieval of three-dimensional tree canopy and shade using terrestrial laser scanning (TLS) data to analyze the cooling effect of vegetation. Agric. For. Meteorol. 217, 22–34.
Landry, S.M., Chakraborty, J., 2009. Street trees and equity: evaluating the spatial distribution of an urban amenity. Environ. Plann. A 41 (11), 2651–2670.
Lee, Hyunjung, Holst, Jutta, Mayer, Helmut, 2013. Modification of human-biometeorologically significant radiant flux densities by shading as local method to mitigate heat stress in summer within urban street canyons. Adv. Meteorol. 1–13.
Li, X., Zhang, C., Li, W., 2015a. Does the visibility of greenery increase perceived safety in urban areas? Evidence from the place pulse 1.0 dataset. ISPRS Int. J. Geo-Inf. 4 (3), 1166–1183.
Li, X., Zhang, C., Li, W., Kuzovkina, Y.A., Weiner, D., 2015b. Who lives in greener neighborhoods? The distribution of street greenery and its association with residents' socioeconomic conditions in Hartford, Connecticut, USA. Urban For. Urban Green. 14 (4), 751–759.
Li, X., Zhang, C., Li, W., Kuzovkina, Y.A., 2016. Environmental inequities in terms of different types of urban greenery in Hartford, Connecticut. Urban For. Urban Green. 18, 163–172.
Li, X., Ratti, C., Seiferling, I., 2017. Mapping urban landscapes along streets using Google Street View. In: International Cartographic Conference. Springer, Cham. pp. 341–356.
Lin, T.P., Tsai, K.T., Hwang, R.L., Matzarakis, A., 2012. Quantification of the effect of thermal indices and sky view factor on park attendance. Landscape Urban Plann. 107 (2), 137–146.
Luber, G., McGeehin, M., 2008. Climate change and extreme heat events. Am. J. Prev. Med. 35 (5), 429–435.
MacFaden, S.W., O'Neil-Dunne, J.P., Royar, A.R., Lu, J.W., Rundle, A.G., 2012. High-resolution tree canopy mapping for New York City using LIDAR and object-based image analysis. J. Appl. Remote Sens. 6 (1), 063567–063571.
McPherson, E.G., Simpson, J.R., 2003. Potential energy savings in buildings by an urban tree planting programme in California. Urban For. Urban Green. 2 (2), 73–86.
Miller, H.J., Tolle, K., 2016. Big data for healthy cities: using location-aware technologies, open data and 3D urban models to design healthier built environments. Built Environ. 42 (3), 441–456.
Mills, G., 2014. Urban climatology: history, status and prospects. Urban Clim. 10, 479–489.
Nowak, D.J., Kuroda, M., Crane, D.E., 2004. Tree mortality rates and tree population projections in Baltimore, Maryland, USA. Urban For. Urban Green. 2 (3), 139–147.
Onishi, A., Cao, X., Ito, T., Shi, F., Imura, H., 2010. Evaluating the potential for urban heat-island mitigation by greening parking lots. Urban For. Urban Green. 9 (4), 323–332.
Otsu, N., 1975. A threshold selection method from gray-level histograms. Automatica 11 (285–296), 23–27.
Raciti, S.M., Hutyra, L.R., Newell, J.D., 2014. Mapping carbon storage in urban trees with multi-source remote sensing data: relationships between biomass, land use, and demographics in Boston neighborhoods. Sci. Total Environ. 500, 72–83.
Ratti, C., Richens, P., 2004. Raster analysis of urban form. Environ. Plann. B: Plann. Des. 31 (2), 297–309.
Richards, D.R., Edwards, P.J., 2017. Quantifying street tree regulating ecosystem services using Google Street View. Ecol. Indic. 77, 31–40.
Salmond, J.A., Tadaki, M., Vardoulakis, S., Arbuthnott, K., Coutts, A., Demuzere, M., McInnes, R.N., 2016. Health and climate related ecosystem services provided by street trees in the urban environment. Environ. Health 15 (1), S36.
Sanusi, R., Johnstone, D., May, P., Livesley, S.J., 2016. Street orientation and side of the street greatly influence the microclimatic benefits street trees can provide in summer. J. Environ. Qual. 45 (1), 167–174.
Steyn, D.G., 1980. The Calculation of View Factors from Fisheye Lens Photographs: Research Note. pp. 254–258.
Watson, I.D., Johnson, G.T., 1987. Graphical estimation of sky view factors in urban environments. J. Climatol. 7 (2), 193–197.
Yuan, C., Norford, L., Ng, E., 2017. A semi-empirical model for the effect of trees on the urban wind environment. Landscape Urban Plann. 168, 84–93.